PAPER *Special Section on Mobile Multimedia Communications*

Link Quality-Based Path Selection Scheme in Millimeter-Wave Broadband Entrance Network for Wireless Heterogeneous Systems

Jaturong SANGIAMWONG[†a)], ***Student Member***, **Katsutoshi TSUKAMOTO**[†], ***Member***, ***and*** **Shozo KOMAKI**[†], ***Fellow***

SUMMARY This paper proposes the constraint availability and bandwidth shortest path (CABSP) selection algorithm and the extension of the adaptive modulation scheme to the CABSP (CABSP-AM) selection algorithm in the millimeter-wave (MMW) broadband entrance network for wireless heterogeneous systems. The CABSP algorithm considers the availability denoted as the quality of the MMW which is severely affected by the rainfall. The CABSP-AM algorithm, moreover, is proposed to further make more efficient use of bandwidth resources by considering the QoS requirements of each class of service in multimedia communication. As the results, the CABSP algorithm yields higher throughput performance than the conventional constraint shortest path (CSP) selection algorithm, but lower than the CABSP-AM algorithm. The spectrum efficiency improvements of the CABSP-AM over the CABSP are about 1.36 and 1.48 fold in case of error sensitive and non-sensitive classes respectively.

key words: *wireless heterogeneous systems, route availability, path selection algorithm, adaptive modulation*

1. Introduction

The proliferation of multimedia communications has motivated extensive research in new broadband services especially the broadband wireless access (BWA) systems offered a tremendous advantage over the wired technologies such as ADSL, CATV and FTTH in point of their rapid deployment with low-cost. The BWA industry has matured to the point at which it now has the IEEE Standard 802.16 for second-generation wireless metropolitan area networks [1]. Fixed wireless access (FWA), one of BWA systems, is expected to play the major role in providing high-speed and flexible services [2]–[4]. In Japan, FWA services at present are provided in the 22, 26 and 38 GHz bands according to the ARIB STD-T58 and STD-T59. However, according to the tremendous of high-speed demand, the new bands should be allocated. As the discussions within WRC-2000, several new bands, e.g., 32, 52 and 55 GHz, have been reserved internationally for the high density fixed service (HDFS) including FWA. In Japan, a new BWA system exploiting 32 GHz band has been developed from today FWA to cope with the rapid growth of demand from now on [5]. As illustrated in Fig. 1, this BWA is developed to provide the seamless broadband Internet access services for the wireless heterogeneous systems including the fixed, nomadic and mobile access services as the entrance network connecting between the base stations (BSs), the center station (CS) and the backbone (BB) network. The concept of the entrance network is similarly investigated in the radio access network (RAN) for the DECT [6] and the 4G mobile communication [7]. In order to support the extension of various novel advanced communications, the entrance network should be simple and independent of technologies of those systems. Hence, instead of using the regenerative repeater, we employ the non-regenerative repeater because it only converts the frequency band, i.e., the entrance network deals with those systems in the wireless physical layer.

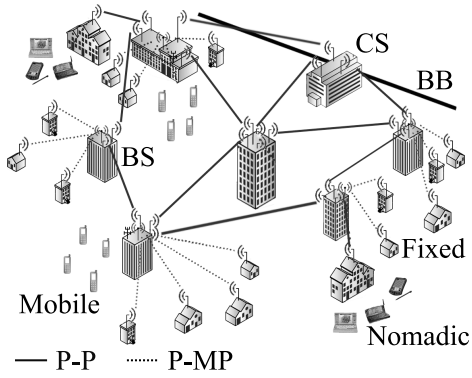

Fig. 1 Millimeter-wave broadband wireless network.

With the implementing of links into P-P (Point-to-Point) mesh-topology as the entrance network, system can support the high-speed communication in high-level of service coverage [8] and is flexible in point of that adaptive routing can be implemented to avoiding the fell down or traffic-congested links. In addition, with the deployment of millimeter-wave (MMW) band, system will meet the large available bandwidth and the reduced size of electronic components. However, its quality is severely affected by rainfall. Hence, unlike the wired system, not only the bandwidth but also the quality of route should be considered. Reference [9] investigated the improvement of availability due to route diversity under rain condition to show the advantage of mesh-topology utilization, but the investigation was simply done in 4 nodes square mesh network with no consideration of routing. The simple route switching from deteriorated route to backup route with the bit error rate (BER) level monitoring was proposed in [10]. In this paper, we consider the availability of route as the quality, and then propose the constraint availability and bandwidth shortest path (CABSP) se-

Manuscript received August 26, 2003.
Manuscript revised October 23, 2003.

[†]The authors are with the Department of Communications Engineering, Graduate School of Engineering, Osaka University, Suita-shi, 565-0871 Japan.
a) E-mail: jaturong@roms.comm.eng.osaka-u.ac.jp

lection algorithm to select the path with the minimum number of hops with abundant availability and bandwidth.

The availability of multi-hop route under rainfall environment, in this paper, is defined as the probability that the rain attenuation of each hop is below a certain allowable value according to the required carrier-to-noise ratio (CNR). In the derivation of the availability, as its definition, the use of rain attenuation distribution is necessary. As expounded in [11]–[13], rain attenuation can be approximated statistically well as the Gamma distribution. The bivariate Gamma distribution was derived for 2 hops route in [9]. This paper theoretically derives the multivariate Gamma distribution taking account of the inter-link spatial correlation for rain attenuation distribution in multi-hop route. Note that the inter-link spatial correlation is considered because of the fact that the rain falls similarly in contiguous links. Moreover, we recommend that not only the inter-link spatial correlation, but also the spatial correlation between routes should be considered by way of the assumption that the rain model in analysis is under the exponentially profiled as expounded in [14].

However, in order to make efficient in the wireless heterogeneous including fixed, nomadic and mobile multimedia communications, various quality of service (QoS) requirements of each class of service should be considered in path selection algorithm. For example, error sensitive traffic should be transmitted over reliable path hence the modulation level will be lowered in the deteriorated route, while error non-sensitive real-time traffic should be transmitted over high-speed path hence it may be transmitted over the deteriorated route with no necessary to lower the modulation level. Therefore, this paper proposes the extension of the adaptive modulation scheme to the CABSP algorithm, called the CABSP-AM, to relieve the quality deterioration due to rainfall and thus make more efficient use of bandwidth resources compared to the CABSP algorithm. The spectrum efficiency of them are compared in this paper. Moreover, the throughput performance between these 2 proposed algorithms and the conventional constraint shortest path (CSP) algorithm, which use the bandwidth as the path selection criterion, are compared.

Remind that our 2 proposed algorithms can also be applied to the regenerative entrance network. Someone may doubt if it is appropriate to use the non-regenerative repeating function because though it can support the heterogeneous wireless systems with ease but it is affected by the cumulative degradation of receiver noise in the non-regenerative repeaters. However, we expect that the efficiency of the non-regenerative method is not so different from that of the regenerative method when the CABSP-AM algorithm is utilized because it seems able to relieve the efficiency deterioration well enough.

The remainder of this paper is organized as follows. Section 2 is devoted to describe the system architecture of the MMW broadband wireless network and the proposed path selection algorithms. In Sect. 3, the multi-hop route availability used as the metric in the proposed algorithms is theoretically derived. Section 4 shows the performance evaluation under various rainfall environments. A conclusion is given in Sect. 5.

2. MMW Broadband Wireless Network

2.1 System Architecture

The architecture of mesh-topology MMW broadband wireless network is illustrated in Fig. 1. Both P-P and P-MP (Point-to-MultiPoint) technologies are deployed to provide services where P-MP links are providing broadband access services, while P-P links are providing the high-bandwidth supply of the broadband entrance network for the wireless heterogeneous systems including the fixed, nomadic and mobile access services. In addition, the non-regenerative repeaters are installed at the BSs in the entrance network. This is because it should deal with the heterogeneous systems in the wireless physical layer to support the extension of various novel advanced systems with ease.

The use of non-regenerative repeating scheme implies that traffic load is transmitted in the physical wireless layer. From this viewpoint, this paper employs the concept of two-plane as shown in the generalized multiprotocol label switching (GMPLS) [15], the control protocol used to set up paths in the IP network, to manage the physical wireless network connections. This control plane is responsible for both routing and signaling to support dynamic provision and restoration of label-forwarding information, and explicit route for each connection between source and destination in whole network. The path is selected by the path manager in control plane. The path manager acquires the state including traffic information from each base station (BS) by using the routing protocol such as the open shortest path first with traffic engineering extension (OSPF-TE) to generate and receive the opaque link-state advertisements (LSAs) [15].

In general, the two well-known on-demand shortest path selection algorithms, the widest shortest path (WSP) and the constraint shortest path (CSP), use the bandwidth as the path selection metric in the wired networks [16]. However, since the use of MMW band in our system, its quality is severely affected by rainfall. Therefore, unlike the wired systems, not only the bandwidth but also the quality should be considered as one of the metrics in the path selection described in details in Sect. 2.2. This paper investigates the quality of MMW route by means of the availability defined as the probability that the rain attenuation is below a certain allowable value according to the required CNR. Generally, the availability requirement is 99.99%, namely an economic "four-nines" of availability. As revealed later in Sect. 3, the availability of each path is calculated by using the information of rainfall assumed to be update periodically from any weather forecast system.

2.2 Path Selection Algorithms

This paper proposes the constraint availability and band-

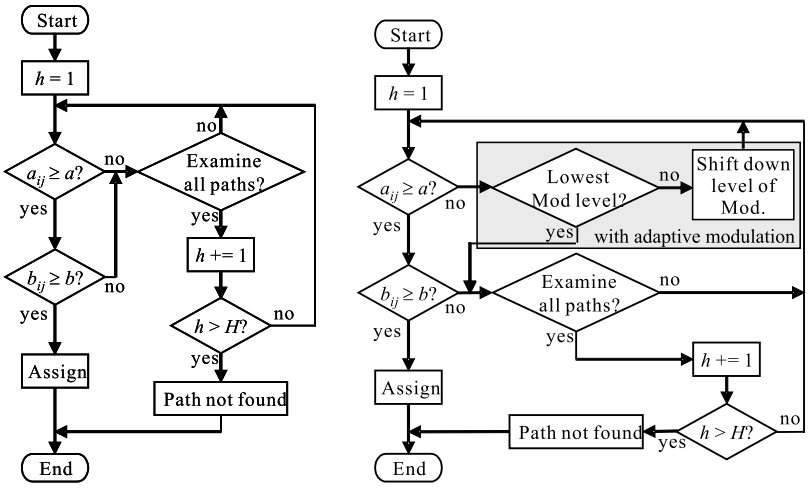

(a) The CABSP. (b) The CABSP-AM.

Fig. 2 Flowchart of path selection algorithms.

width shortest path (CABSP) selection algorithm to select the path with the minimum number of hops with abundant availability and bandwidth. The flowchart of the proposed CABSP selection algorithm is shown in Fig. 2(a). The CABSP selection algorithm selects the path with the minimum number of hops with abundant availability and bandwidth. This algorithm iteratively identifies the possible path from source to destination in increasing order of hop count h with a maximum of H hops. The route that does not satisfy the availability requirement a or the bandwidth requirement b is eliminated. If no one of paths with hop count of h satisfies the availability and bandwidth requirement, the paths with next order of hop count will be considered. On the other hand, if there are multiple paths with the same path quality, one of them is randomly selected. When the shortest possible path is discovered, it is assigned as the explicit route, and then the signaling protocol, either the constraint-based routing label distribution protocol (CR-LDP) or the resource reservation protocol with traffic engineering extension (RSVP-TE) [15], is responsible for establishing forwarding state and reserve resource along the route.

In the CABSP algorithm using the fixed level of modulation of 256QAM, the elimination of route that does not satisfy the availability requirement implies that the route detour avoiding the heavy rain zone is done. For that matter, this algorithm is not bandwidth-efficient. Therefore, this paper proposes the extension of the adaptive modulation scheme to the CABSP (CABSP-AM) selection algorithm as shown in the shadowed box in Fig. 2(b) in order to relieve the performance deterioration due to rainfall and thus make more efficient use of bandwidth resources. The modulation levels used in this algorithm are 256/64/16QAM and QPSK. Before eliminating the low-level of availability route, the modulation level is shifted down, i.e., lower the level of CNR requirement for the threshold required bit error rate (BER), until it meets the availability requirement a, and it will be assigned as the explicit route if it also meets the bandwidth requirement b. Moreover, in the CABSP-AM algorithm, the class of service is also considered in point of that the error sensitive class needs larger required CNR than the error non-sensitive class, which we set the threshold of required BER as 10^{-8} and 10^{-4} respectively.

Note that the proposed path selection algorithms can be applied to not only the non-regenerative entrance network utilized in our heterogeneous systems but also the regenerative entrance network. The calculation of the availability of multi-hop route, used in our proposed path selection algorithms, is revealed in next section.

3. Derivation of Multi-hop Route Availability

Let us start the derivation of the multivariate Gamma distribution with the use of the multivariate Nakagami m-distribution [17] because of the fact about the Nakagami m-distribution and Gamma distribution that if the envelope is Nakagami m-distributed, the corresponding instantaneous power is Gamma distributed. When the rain rate of n hops each are assumed to be $R_1, R_2, ..., R_n$, respectively, the joint PDF of multihop rain rate distribution can be derived as

$$\begin{aligned} f(R_1, R_2, ..., R_n) = & \frac{\prod_{i=1}^{n} \beta_i \cdot (\beta_1 R_1 \beta_n R_n)^{\frac{(\nu-1)}{2}}}{\Gamma(\nu) \cdot \prod_{i=1}^{n-1}(1-\rho_{i,i+1})} \\ & \cdot \frac{1}{\prod_{i=1}^{n-1}(\rho_{i,i+1})^{\frac{(\nu-1)}{2}}} \cdot \exp\left\{ -\left[\frac{\beta_1 R_1}{1-\rho_{1,2}} \right.\right. \\ & \left.\left. + \frac{\beta_n R_n}{1-\rho_{n-1,n}} + \sum_{i=2}^{n-1} \frac{(1-\rho_{i-1,i+1})\beta_i R_i}{(1-\rho_{i-1,i})(1-\rho_{i,i+1})} \right] \right\} \\ & \cdot \prod_{i=1}^{n-1} I_{\nu-1}\left[\frac{2\sqrt{\rho_{i,i+1}\beta_i R_i \beta_{i+1} R_{i+1}}}{1-\rho_{i,i+1}} \right] \end{aligned} \quad (1)$$

where ν and β_i are the parameters of rain rate distribution. $I_{\nu-1}(x)$ is the modified Bessel function of the first kind and of order $\nu - 1$. $\rho_{j,k}$ is the inter-link spatial correlation of

rain distribution between radio link j and k. While parameter ν depends on the geographical location, parameter β_i is denoted as

$$\beta_i = \nu \cdot G/R_{75_i} \tag{2}$$

$$\begin{aligned}\log G = {} & 0.97876 - 0.68355(\log \nu) \\ & + 0.1392(\log \nu)^2 + 0.069921(\log \nu)^3 \\ & + 0.016012(\log \nu)^4 + 0.0018985(\log \nu)^5\end{aligned} \tag{3}$$

where R_{75_i} is the 0.0075% value of the distribution of one hour rain rate, i.e., 0.0075% of rain rate is exceed the R_{75} value of link i [13]. In addition, the inter-link spatial correlation between two contiguous radio links, $\rho_{j,k}$, can be given by

$$\rho_{i,i+1} = \frac{\int_0^{D_i}\int_0^{D_{i+1}} \rho\left(\|x\vec{i}_i - y\vec{i}_{i+1}\|\right) dydx}{2\sqrt{\tau(D_i)\cdot\tau(D_{i+1})}} \tag{4}$$

$$\rho(x) = \exp\left(-\alpha_{sc}\sqrt{x}\right) \tag{5}$$

$$\begin{aligned}\tau(x) = {} & \frac{2}{\alpha_{sc}^2}\cdot\left[x + 2\cdot\left\{x + \frac{3}{\alpha_{sc}}\left(\sqrt{x} + \frac{1}{\alpha_{sc}}\right)\right\}\right. \\ & \left.\cdot\exp\left(-\alpha_{sc}\sqrt{x}\right) - \frac{6}{\alpha_{sc}^2}\right]\end{aligned} \tag{6}$$

where $\vec{i}_i$ and $\vec{i}_{i+1}$ are the unit vector of link i and $i+1$, D_i and D_{i+1} are the distance of link i and $i+1$ respectively. α_{sc} is the spatial correlation parameter [12]. Note that, since the spatial correlation structure is the exponential relationship, the inter-link spatial correlation coefficient, $\rho_{j,k}$, appeared in Eq. (1) can be expressed by simple Marcov chain model as

$$\rho_{j,k} = \prod_{i=j}^{k-1}\rho_{i,i+1} \tag{7}$$

From the power-law relationship by ITU-R recommendation [18], the rain attenuation of distance D propagated wave can be expressed as

$$Z = k\int_0^D R^\alpha dx \tag{8}$$

where R is the rain rate in mm/h, k and α are power-law parameters, which depend on frequency, raindrop size, rain temperature and polarization [18]–[20]. From Eq. (8), the rain attenuation, Z [dB], can also be approximated well as Gamma distribution [12]. Therefore, when the rain attenuation of n hops each are $Z_1, Z_2, ..., Z_n$, respectively, the joint PDF of multihop rain attenuation distribution can be written as

$$\begin{aligned}f(Z_1, Z_2, ..., Z_n) = {} & \frac{\prod_{i=1}^n \beta_{z_i}\cdot(\beta_{z_1}Z_1\beta_{z_n}Z_n)^{\frac{(\nu_z-1)}{2}}}{\Gamma(\nu_z)\cdot\prod_{i=1}^{n-1}(1-\rho_{z_{i,i+1}})} \\ & \cdot\frac{1}{\prod_{i=1}^{n-1}(\rho_{z_{i,i+1}})^{\frac{(\nu_z-1)}{2}}}\cdot\exp\left\{-\left[\frac{\beta_{z_1}Z_1}{1-\rho_{z_{1,2}}}\right.\right. \\ & \left.\left.+\frac{\beta_{z_n}Z_n}{1-\rho_{z_{n-1,n}}} + \sum_{i=2}^{n-1}\frac{(1-\rho_{z_{i-1,i+1}})\beta_{z_i}Z_i}{(1-\rho_{z_{i-1,i}})(1-\rho_{z_{i,i+1}})}\right]\right\}\end{aligned}$$

$$\cdot\prod_{i=1}^{n-1} I_{\nu_z-1}\left[\frac{2\sqrt{\rho_{z_{i,i+1}}\beta_{z_i}Z_i\beta_{z_{i+1}}Z_{i+1}}}{1-\rho_{z_{i,i+1}}}\right] \tag{9}$$

where ν_z and β_{z_i} are the parameters of rain attenuation distribution, and related with the parameters of rain rate distribution, ν and β_i, as

$$\nu_z = \left[\frac{1}{n}\cdot\sum_{i=1}^n\frac{D_i^2}{\delta_i}\right]\cdot\frac{\left\{\frac{\Gamma(\nu+\alpha)}{\Gamma(\nu)}\right\}^2}{\left\{\frac{\Gamma(\nu+2\alpha)}{\Gamma(\nu)} - \frac{\Gamma(\nu+\alpha)^2}{\Gamma(\nu)^2}\right\}} \tag{10}$$

$$\beta_{z_i} = \frac{D_i}{\delta_i\cdot k}\cdot\frac{\left\{\frac{\Gamma(\nu+\alpha)}{\Gamma(\nu)}\cdot{\beta_i}^\alpha\right\}}{\left\{\frac{\Gamma(\nu+2\alpha)}{\Gamma(\nu)} - \frac{\Gamma(\nu+\alpha)^2}{\Gamma(\nu)^2}\right\}} \tag{11}$$

$$\delta_i = 2\cdot\tau(D_i) \tag{12}$$

Note that, the inter-link spatial correlation of rain attenuation, $\rho_{z_{j,k}}$, is set to be [12]

$$\rho_{z_{j,k}} = 0.9\cdot\rho_{j,k} \tag{13}$$

In the derivation of the multihop route availability, we define the maximum allowable rain attenuation of n hops each are $L_{R_1}, L_{R_2}, ..., L_{R_n}$ [dB], respectively, hence, the availability can be computed as the joint CDF

$$\begin{aligned}F(L_{R_1}, L_{R_2}, ..., L_{R_n}) = {} & \int_0^{L_{R_n}}\int_0^{L_{R_{n-1}}}\cdots\int_0^{L_{R_1}} \\ & \cdot f(Z_1, Z_2, ..., Z_n)dZ_1dZ_2\ldots dZ_n\end{aligned} \tag{14}$$

where L_{R_i} [dB] is given by

$$\begin{aligned}L_{R_i} = {} & P_T + 2G(0) - L(D_i) - \gamma_0 D_i \\ & - 10\log(i) - N - CNR_{req}\end{aligned} \tag{15}$$

where P_T is the transmitted power, $G(0)$ is the antenna gain, $L(D_i)$ is the path loss, γ_0 is the atmosphere absorption factor, N is the thermal noise, and CNR_{req} is the required CNR.

After the derivation is completed by integrating all components in Eq. (14), we obtain (see Appendix for the derivation in details)

$$\begin{aligned}F(L_{R_1}, L_{R_2}, ..., L_{R_n}) = {} & \frac{1}{\Gamma(\nu_z)} \\ & \cdot\sum_{j_1,j_2,...,j_{n-1}=0}^{\infty}\left\{\frac{\prod_{i=1}^{n-1}\left(\rho_{z_{i,i+1}}\right)^{j_i}\cdot\left(1-\rho_{z_{1,2}}\right)^{(\nu_z+j_2)}}{\prod_{i=1}^{n-1}j_i!\Gamma(\nu_z+j_i)}\right. \\ & \cdot\frac{\prod_{i=2}^{n-2}\left(1-\rho_{z_{i,i+1}}\right)^{(\nu_z+j_{i-1}+j_{i+1})}}{\prod_{i=2}^{n-1}\left(1-\rho_{z_{i-1,i+1}}\right)^{(\nu_z+j_{i-1}+j_i)}} \\ & \cdot\left(1-\rho_{z_{n-1,n}}\right)^{\nu_z+j_{n-2}}\cdot\gamma\left(\nu_z+j_1, \frac{\beta_{z_1}L_{R_1}}{1-\rho_{z_{1,2}}}\right) \\ & \cdot\prod_{i=2}^{n-1}\gamma\left(\nu_z+j_{i-1}+j_i, \frac{\left(1-\rho_{z_{i-1,i+1}}\right)\beta_{z_i}L_{R_i}}{\left(1-\rho_{z_{i-1,i}}\right)\left(1-\rho_{z_{i,i+1}}\right)}\right) \\ & \left.\cdot\gamma\left(\nu_z+j_{n-1}, \frac{\beta_{z_n}L_{R_n}}{1-\rho_{z_{n-1,n}}}\right)\right\}\end{aligned} \tag{16}$$

4. Performance Evaluation under Rainfall Environments

The analysis model is illustrated in Fig. 3. The four BSs ⓐ–ⓓ and the CS ⓔ each, arranged into pentagonal mesh-topology, are established connections with P-P links as the non-regenerative entrance network. Note that, in Sect. 3, only the spatial correlations between hops in route were taken into account. However, the spatial correlation between routes should also be considered by way of the use of exponentially profiled rain cells expounded in [14]. The analysis model is under the assumption of a five exponentially profiled R_{75} rain cells which each have the same peak rate environment. Since the entrance network deploys the P-P MMW links, it is assumed to be the line-of-sight (LOS) under AWGN channel. Table 1 lists the parameters used in the calculations. For the sake of simplicity, the calculation is done in the case of the uniform traffic, i.e., $\lambda_i = \lambda;\ \forall i \in \mathbb{BS}$ where $\mathbb{BS}$ is the set of the base stations.

Figure 4 compares the spectrum efficiency between the CABSP and the CABSP-AM algorithm. The spectrum efficiency is defined as $\eta = \mu_{tot}/xB$ [bps/Hz]; $x = \sum_i \lambda_i/\lambda$ where μ_{tot} is the total traffic capacity of network, B is the bandwidth of radio link. Note that x becomes the number of BSs in the case of uniform traffic. From Fig. 4, we can see that the spectrum efficiency is improved when the peak R_{75} rate exceeds 42 mm/h. In the case of peak R_{75} rate is 76.5 mm/h, the CABSP-AM selection scheme can improve the spectrum efficiency in case of the error non-sensitive and error sensitive classes over that of the CABSP selection scheme around 1.25 and 1.33 fold, respectively.

Moreover, the spectrum efficiency calculation is done in the case of using regenerative repeaters in order to compare the performance with the case of using non-regenerative repeaters. The results are shown in Fig. 5. Compared with Fig. 4, we can see that the spectrum efficiency of the regenerative method is better than that of the non-regenerative method in the region of peak R_{75} rate of 98–112 mm/h when using the CABSP algorithm. On the other hand, when the CABSP-AM algorithm is utilized, the spectrum efficiency of the non-regenerative method is not so different from that of the regenerative method. Thus it is made clear that the drawback of noise accumulation in non-regenerative repeaters is not significant when using the CABSP-AM algorithm.

Figure 6 compares the throughput performance, denoted by the number of success received traffic, between the conventional CSP, the CABSP and the CABSP-AM algorithm as a function of the normalized aggregated load, which

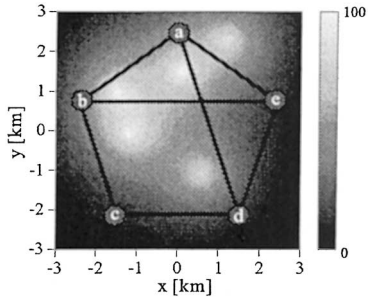

(a) The bird's eyes view.

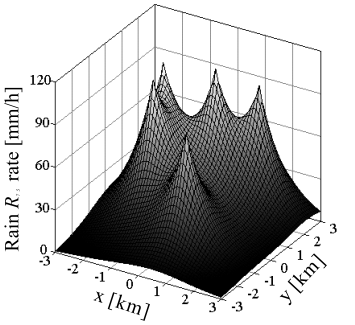

(b) The R_{75} rate (peak R_{75} rate of 76.5 mm/h).

Fig. 3 Analysis model.

Table 1 Parameters used in calculations.

Carrier frequency	f_c	32 GHz
Bandwidth	B	240 MHz
Transmitted power	P_T	30 dBm
Antenna gain	$G(o)$	42 dBi
Noise figure	F	8 dB
Rolloff factor	α_{ro}	0.15
Atmosphere absorption factor	γ_0	0.11 dB/km
Rain rate parameter	ν	0.005
Spatial correlation parameter	α_{sc}	0.3

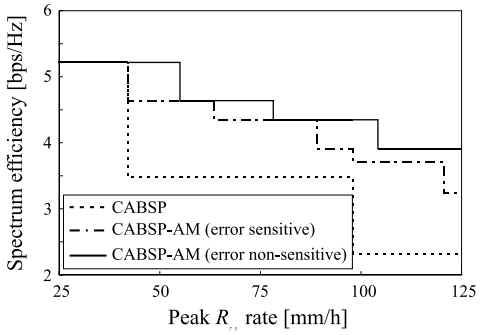

Fig. 4 Spectrum efficiency.

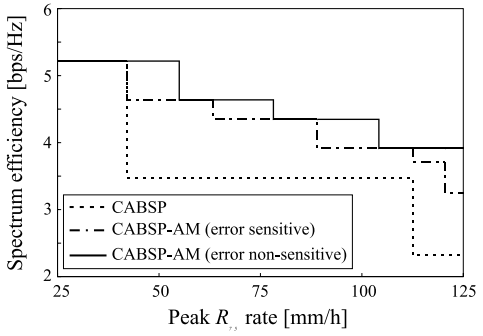

Fig. 5 Spectrum efficiency (regenerative).

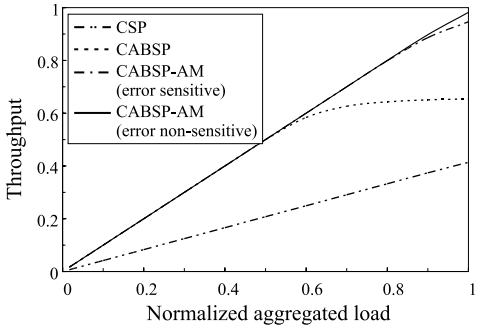

(a) Peak R_{75} rate of 76.5 mm/h.

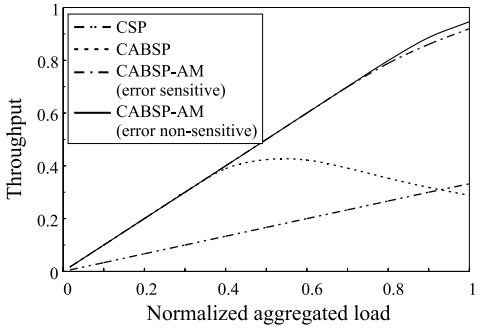

(b) Peak R_{75} rate of 100 mm/h.

Fig. 6 Throughput performance (uniform traffic).

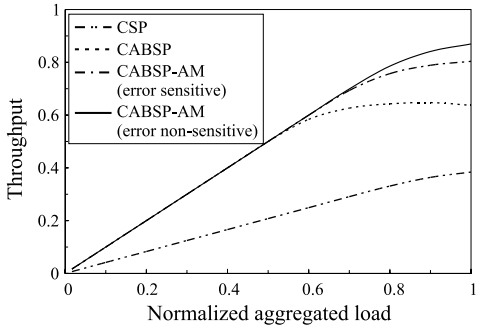

(a) Peak R_{75} rate of 76.5 mm/h.

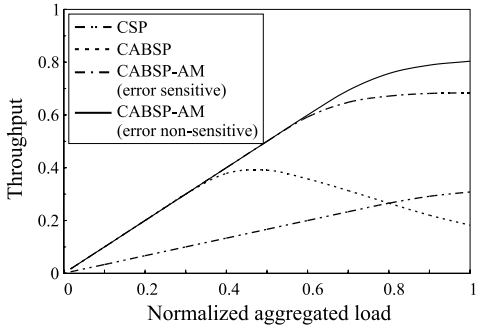

(b) Peak R_{75} rate of 100 mm/h.

Fig. 7 Throughput performance (skew traffic).

becomes 1 in the case of the total generated load equals the total traffic capacity of network when all links use 256QAM, in the case of peak R_{75} rates are 76.5 and 100 mm/h. The CSP method yields the throughput less than 0.3–0.4 since it routes traffic with no regard of link deterioration due to rain. The CABSP method yields higher throughput than the CSP method because it routes traffic avoiding the high-loss link. However, the throughput becomes saturated when traffic load exceeds 0.6 when peak R_{75} rates is 76.5 mm/h, and first increases and reaches a peak at the traffic load of 0.5 and then starts to decrease if the load increases further when peak R_{75} rates is 100 mm/h. On the other hand, the CABSP-AM method gives higher throughput than the CABSP method because it makes more efficient use of bandwidth. The throughput improvement by the CABSP-AM method becomes evident when the rain rate increases.

In addition, the throughput performance comparison in the case of skew traffic with condition of $\lambda_i = \lambda;\ \forall i_{i \neq ⓑ} \in \mathbb{BS}$ and $\lambda_{ⓑ} = 2\lambda$ is shown in Fig. 7. Compared with the case of uniform traffic, it is obvious that the throughput performance of the CABSP algorithm becomes worse particularly in the case of peak R_{75} rates is 100 mm/h. On the other hand, the CABSP-AM algorithm yields higher throughput than other algorithms in both rainfall conditions.

In order to assure the superiority of the proposed algorithm, the analysis is done under the various rainfall conditions by randomly locating the peak point of five rain cells which have same peak R_{75} rate of 100 mm/h. Figure 8 shows the cumulative distribution of the spectrum efficiency. We can see that the CABSP-AM algorithm improves the spectrum efficiency compared to the CABSP algorithm. Table 2

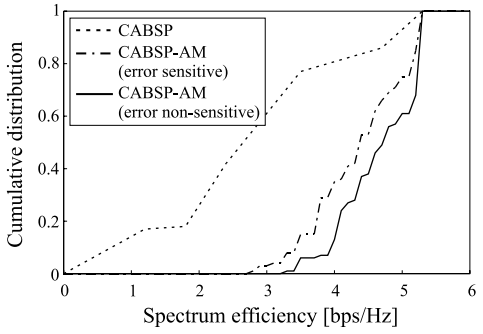

Fig. 8 Cumulative distribution of the spectrum efficiency (uniform traffic).

Table 2 Spectrum efficiency (uniform traffic).

	Mean [bps/Hz]	σ [bps/Hz]
CABSP	3.14	1.31
CABSP-AM (error sensitive)	4.34	0.68
CABSP-AM (error non-sensitive)	4.64	0.56

lists the mean and the standard deviation σ of the spectrum efficiency. The CABSP-AM algorithm can improve the spectrum efficiency in case of the error non-sensitive and sensitive classes over that of the CABSP algorithm about 1.38 and 1.48 fold, respectively. The less σ value of the CABSP-AM algorithm indicates that it can smooth out the effect from the rainfall fluctuations.

Figure 9 shows the cumulative distribution of the spectrum efficiency in the case of skew traffic ($\lambda_i = \lambda;\ \forall i_{i \neq ⓑ} \in$

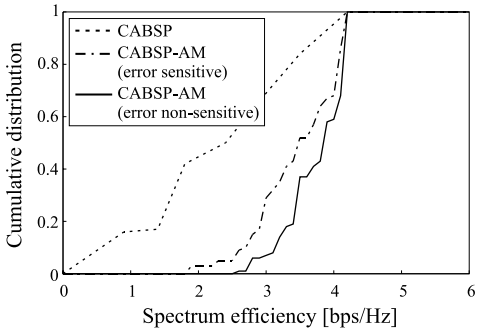

Fig. 9 Cumulative distribution of the spectrum efficiency (skew traffic).

Table 3 Spectrum efficiency (skew traffic).

	Mean [bps/Hz]	σ [bps/Hz]
CABSP	2.53	1.12
CABSP-AM (error sensitive)	3.45	0.61
CABSP-AM (error non-sensitive)	3.74	0.43

$\mathbb{BS}$ and $\lambda_{ⓑ} = 2\lambda$). The results assure the superiority of the CABSP-AM algorithm in point of that it is efficient even in the skew traffic conditions. Table 3 lists the mean and the standard deviation σ of the spectrum efficiency. The CABSP-AM algorithm can improve the spectrum efficiency in case of the error non-sensitive and sensitive classes over that of the CABSP algorithm about 1.36 and 1.48 fold respectively.

5. Conclusion

This paper has proposed the CABSP and the CABSP-AM selection algorithms for the P-P mesh-topology MMW broadband entrance network for wireless heterogeneous systems. The CABSP selection algorithm was proposed to taking account of the quality of the MMW which is severely affected by the rainfall. The CABSP-AM selection algorithm, moreover, was proposed to further make more efficient use of bandwidth resources with consideration of the QoS requirement of each class of service in multimedia communication.

The analysis model seems to be simple then the degree of freedom in path selection is small, i.e., few of path candidates, hence the efficiency of the proposed algorithm in this model assures that it also work efficient in the practical network. As the results, the CABSP algorithm yields higher throughput performance than the conventional constraint shortest path (CSP) selection algorithm, but lower than the CABSP-AM algorithm. The cumulative distribution of the spectrum efficiency indicated that the CABSP-AM algorithm makes the superiority over the CABSP algorithm in any rainfall and traffic condition, and the spectrum efficiency improvements of the CABSP-AM algorithm over the CABSP algorithm are about 1.36 and 1.48 fold in case of error sensitive and non-sensitive classes respectively. In addition, the CABSP-AM method can relieve the drawback of noise accumulation in the non-regenerative entrance network for heterogeneous systems, and thus make its efficiency not so different from that of case using the regenerative repeaters.

Acknowledgement

This paper is partially supported by the Grants-in-Aid for Scientific Research (B) No.14350202, from the Japan Society for the Promotion of Science. The authors would like to thank Dr. Hiroyo Ogawa and Dr. Yozo Shoji, CRL, Japan, for their valuable advices.

References

[1] C. Eklund, R.B. Marks, K.L. Stanwood, and S. Wang, "IEEE standard 802.16: A technical overview of the WirelessMAN^{TM} air interface for broadband wireless access," IEEE Commun. Mag., vol.40, no.6, pp.98–107, June 2002.

[2] H. Bolcskei, A.J. Paulraj, K.V.S. Hari, R.U. Nabar, and W.W. Lu, "Fixed broadband wireless access: State of the art, challenges, and future directions," IEEE Commun. Mag., vol.39, no.1, pp.100–108, Jan. 2001.

[3] W. Webb, "Broadband fixed wireless access as a key component of the future integrated communications environment," IEEE Commun. Mag., vol.39, no.9, pp.115–121, Sept. 2001.

[4] Fixed Wireless Access Systems Development in ARIB, "Study report for fixed wireless access system," (in Japanese) June 1999.

[5] K. Tsukamoto, S. Komaki, K. Takanashi, A. Kanazawa, Y. Shoji, H. Ogawa, M. Yoshikawa, S. Asami, M. Kaneta, Y. Suzuki, T. Fukagawa, and Y. Serizawa, "Development of gigabit millimeter-wave broadband wireless access systems—(1) System overview," Proc. 5th TSMMW, pp.105–108, March 2003.

[6] M. Celidonio and D.D. Zenobio, "A wideband two-layer radio access network using DECT technology in the uplink," IEEE Commun. Mag., vol.37, no.10, pp.76–81, Oct. 1999.

[7] T. Otsu, Y. Aburakawa, and Y. Yamao, "Multi-hop wireless link system for new generation mobile radio access networks," IEICE Trans. Commun., vol.E85-B, no.8, pp.1542–1551, Aug. 2002.

[8] P. Whitehead, "Mesh networks: A new architecture for broadband wireless access systems," IEEE RAWCON2000, pp.43–46, May 2000.

[9] S. Nomoto, K. Nakama, and Y. Kishi, "Route diversity effect of mesh network taking account of space correlation of rainfall," IEICE Technical Report, RCS2001-57, June 2001.

[10] M. Yokobori, T. Kawakami, Y. Suzuki, K. Takanashi, and H. Ogawa, "Development of gigabit millimeter-wave broadband wireless access systems—(2) Study on reliability of the path control method," Proc. 5th TSMMW, pp.109–112, March 2003.

[11] K. Morita and I. Higuchi, "Statistical studies on electromagnetic wave attenuation due to rain," (in Japanese) NTT R&D Review, vol.19, no.1, pp.97–150, 1970.

[12] K. Morita and I. Higuchi, "Estimation of differential rain attenuation on adjacent millimeter wave links," (in Japanese) NTT R&D Review, vol.25, no.2, pp.467–479, 1976.

[13] Y. Hosoya, O. Sasaki, T. Shirato, and K. Morita, "Estimation for characteristics of 20 GHz band propagation through rain," (in Japanese) NTT R&D Review, vol.33, no.6, pp.1221–1231, 1984.

[14] A. Paraboni, G. Masini, and A. Elia, "The effect of precipitation on microwave LMDS networks—Performance analysis using a physical raincell model," IEEE J. Sel. Areas Commun., vol.20, no.3, pp.615–619, April 2002.

[15] E. Mannie, et al., "Generalized multi-protocol label switching (GMPLS) architecture," Internet Draft, draft-ietf-ccamp-gmpls-architecture-04.txt, Feb. 2003.

[16] Y.D. Lin, N.B. Hsu, and R.H. Hwang, "QoS routing granularity in MPLS networks," IEEE Commun. Mag., vol.40, no.6, pp.98–107, June 2002.
[17] M. Nakagami and Y. Miyagaki, "Improvement of the channel quality by automatic protection switching for microwave radio systems," (in Japanese) NTT R&D Review, vol.16, no.7, pp.1293–1315, 1967.
[18] ITU-R Recommendation P.838, "Specific attenuation model for rain for use in prediction methods," 1992.
[19] W. Zhang and N. Moayari, "Power-law parameter of rain specific attenuation," Doc. no.IEEE 802.16cc-99/24, Nov. 1999.
[20] W. Zhang and N. Moayari, "Recommendation: Use of various raindrop size distributions for different geographical locations in calculating the rain specific attenuation," Doc. no.IEEE 802.16cc-99/41, Jan. 2000.

Appendix

From Eq. (9) and Eq. (14), Substituting $I_{\nu_z-1}(x)$ with a series expansion in terms of Gamma functions

$$I_{\nu_z-1}(x) = \left(\frac{x}{2}\right)^{\nu_z-1} \cdot \sum_{n=0}^{\infty} \frac{(x/2)^{2n}}{n!\Gamma(\nu_z+n)}, \tag{A·1}$$

we obtain

$$\begin{aligned} F(L_{R_1}, L_{R_2}, ..., L_{R_n}) &= \int_0^{L_{R_n}} \int_0^{L_{R_{n-1}}} \cdots \int_0^{L_{R_2}} \\ &\frac{\prod_{i=1}^{n}(\beta_{z_i})^{\nu_z} \cdot \prod_{i=2}^{n}(Z_i)^{\nu_z-1}}{\Gamma(\nu_z) \cdot \prod_{i=1}^{n-1}(1-\rho_{z_{i,i+1}})^{\nu_z}} \cdot \exp\left\{ -\left[\right.\right. \\ &\left.\left. \frac{\beta_{z_n} Z_n}{1-\rho_{z_{n-1,n}}} + \sum_{i=2}^{n-1} \frac{(1-\rho_{z_{i-1,i+1}})\beta_{z_i} Z_i}{(1-\rho_{z_{i-1,i}})(1-\rho_{z_{i,i+1}})} \right]\right\} \\ &\cdot \prod_{i=2}^{n-1}\left[\sum_{j_i=0}^{\infty} \frac{\left(\rho_{z_{i,i+1}} \beta_{z_i} Z_i \beta_{z_{i+1}} Z_{i+1}\right)^{j_i}}{j_i!\Gamma(\nu_z+j_i)\left(1-\rho_{z_{i,i+1}}\right)^{2j_i}} \right] \\ &\cdot \left[\sum_{j_1=0}^{\infty} \frac{\left(\rho_{z_{1,2}} \beta_{z_1} \beta_{z_2} Z_2\right)^{j_1}}{j_1!\Gamma(\nu_z+j_1)\left(1-\rho_{z_{1,2}}\right)^{2j_1}} \cdot \int_0^{L_{R_1}} \right. \\ &\left. Z_1{}^{\nu_z+j_1-1} \exp\left(-\frac{\beta_{z_1} Z_1}{1-\rho_{z_{1,2}}}\right) dZ_1 \right] dZ_2 dZ_3 \ldots dZ_n \end{aligned} \tag{A·2}$$

The relationship of the incomplete Gamma function

$$\int_0^u x^{\nu_z-1} e^{-\mu x} dx = \mu^{-\nu_z} \cdot \gamma(\nu_z, \mu u) \tag{A·3}$$

is then taken into Eq. (A·2). It can be rewritten as

$$\begin{aligned} F(L_{R_1}, L_{R_2}, ..., L_{R_n}) &= \int_0^{L_{R_n}} \int_0^{L_{R_{n-1}}} \cdots \int_0^{L_{R_2}} \\ &\frac{\prod_{i=1}^{n}(\beta_{z_i})^{\nu_z} \cdot \prod_{i=2}^{n}(Z_i)^{\nu_z-1}}{\Gamma(\nu_z) \cdot \prod_{i=1}^{n-1}(1-\rho_{z_{i,i+1}})^{\nu_z}} \cdot \exp\left\{ -\left[\right.\right. \\ &\left.\left. \frac{\beta_{z_n} Z_n}{1-\rho_{z_{n-1,n}}} + \sum_{i=2}^{n-1} \frac{(1-\rho_{z_{i-1,i+1}})\beta_{z_i} Z_i}{(1-\rho_{z_{i-1,i}})(1-\rho_{z_{i,i+1}})} \right]\right\} \\ &\cdot \prod_{i=2}^{n-1}\left[\sum_{j_i=0}^{\infty} \frac{\left(\rho_{z_{i,i+1}} \beta_{z_i} Z_i \beta_{z_{i+1}} Z_{i+1}\right)^{j_i}}{j_i!\Gamma(\nu_z+j_i)\left(1-\rho_{z_{i,i+1}}\right)^{2j_i}} \right] \\ &\cdot \left[\sum_{j_1=0}^{\infty} \frac{\left(\rho_{z_{1,2}} \beta_{z_2} Z_2\right)^{j_1}}{j_1!\Gamma(\nu_z+j_1)\left(1-\rho_{z_{1,2}}\right)^{j_1}} \right. \\ &\left. \cdot \gamma\left(\nu_z+j_1, \frac{\beta_{z_1} L_{R_1}}{1-\rho_{z_{1,2}}}\right) \right] dZ_2 dZ_3 \ldots dZ_n \end{aligned} \tag{A·4}$$

Similarly, the derivation is done from then on. Finally, Eq. (16) is obtained.

Jaturong Sangiamwong was born in Chachoengsao, Thailand on June 1, 1980. He received the B.E. degree in Electrical Engineering from Chulalongkorn University, Bangkok, Thailand, in 2000, and the M.E. degree in Communications Engineering from Osaka University, Osaka, Japan, in 2002. He is currently pursuing the Ph.D. degree at Osaka University. He is engaged in the research on broadband wireless communication systems.

Katsutoshi Tsukamoto was born in Shiga, Japan on October 7, 1959. He received B.E., M.E. and Ph.D. degrees in Communications Engineering from Osaka University, in 1982, 1984 and 1995, respectively. He is currently an Associate Professor in the Department of Communications Engineering at Osaka University, engaged in the research on radio and optical communication systems. He is a member of IEEE and ITE. He was awarded the Paper Award of IEICE, Japan in 1996.

Shozo Komaki was born in Osaka, Japan in 1947. He received B.E., M.E. and Ph.D. degrees in Communications Engineering from Osaka University, in 1970, 1972 and 1983, respectively. In 1972, he joined the NTT Radio Communication Labs., where he has engaged in repeater development for a 20-GHz digital radio system, and 16-QAM and 256-QAM systems. In 1990, he moved to Osaka University, Faculty of Engineering, and is engaged in research on radio and optical communication systems. He is currently a Professor of Osaka University. Dr. Komaki is a senior member of the Institute of Television Engineering of Japan (ITE). He was awarded the Paper Award and the Achievement Award of IEICE, Japan in 1977 and 1994 respectively.